Anomalous reduction in domain wall displacement at the morphotropic phase boundary of the piezoelectric alloy system $PbTiO_3$-$BiScO_3$

Dipak Kumar Khatua,[1] Lalitha K. V.,[1] Chris M. Fancher,[2] Jacob L. Jones,[2] and Rajeev Ranjan[1,*]
[1]*Department of Materials Engineering, Indian Institute of Science, Bangalore 560012, India*
[2]*Department of Materials Science and Engineering, North Carolina State University, Raleigh, North Carolina 27695, USA*
(Received 5 June 2015; revised manuscript received 4 February 2016; published 2 March 2016)

A comparative study of field-induced domain switching and lattice strain was carried out by *in situ* electric-field-dependent high-energy synchrotron x-ray diffraction on a morphotropic phase boundary (MPB) and a near-MPB rhombohedral/pseudomonoclinic composition of a high-performance piezoelectric alloy $(1-x)PbTiO_3$-$(x)BiScO_3$. It is demonstrated that the MPB composition showing large $d_{33} \sim 425\ pC/N$ exhibits significantly reduced propensity of field-induced domain switching as compared to the non-MPB rhombohedral composition ($d_{33} \sim 260\ pC/N$). These experimental observations contradict the basic premise of the martensitic-theory-based explanation which emphasizes on enhanced domain wall motion as the primary factor for the anomalous piezoelectric response in MPB piezoelectrics. Our results favor field-induced structural transformation to be the primary mechanism contributing to the large piezoresponse of the critical MPB composition of this system.

DOI: 10.1103/PhysRevB.93.104103

I. INTRODUCTION

Morphotropic phase boundary (MPB) ferroelectrics are widely used as actuators, sensors, and transducers by virtue of their exceptionally large piezoelectric response. A first intuitive explanation for the large electromechanical response was attributed to the availability of a large number of domain variants, which was supposed to enable efficient poling of the specimen [1]. This idea received theoretical support from a Devonshire-Ginzburg-Landau-based multiscale calculation which predicted enhanced domain switching in MPB systems [2]. The same scenario is considered to be applicable in single phase low-symmetry ferroelectrics [2]. In contrast, first-principles [3,4] and phenomenological free-energy calculations [5–7] have shown a correlation between anisotropic flattening of a free-energy profile and polarization rotation, assisted by low-symmetry phases as the fundamental mechanism for an enhanced piezoelectric response in ferroelectrics [3–10]. Martensitic-based theory on the other hand, attributes the large piezoelectric response of the MPB systems to enhanced density and mobility of domain walls [11–16]. *In situ* electric-field diffraction experiments enable direct estimation of domain switching and lattice strain in ferroelectrics [17–23]. Ghosh *et al.* have shown that the relatively enhanced dielectric and piezoelectric responses of polycrystalline $BaTiO_3$ in the grain size range of $\sim$1 to 2 μm is associated with an enhanced domain wall displacement [24]. The authors concluded this by comparing the domain switching fraction in $BaTiO_3$ ceramics of different grain sizes and found it to be largest in the size range of 1 to 2 μm. Apart from studying domain switching, an *in situ* field-dependent diffraction experiment can also ascertain the occurrence of field-induced interferroelectric transformation, if any. However, the combined effect of preferred orientation and severe overlapping of Bragg peaks corresponding to the different phases makes structural analysis very challenging. Using a special diffraction geometry to avoid a field-induced preferred orientation effect, Hinterstein *et al.* have shown evidence of field-induced tetragonal to rhombohedral/monoclinic transformation in a soft lead zirconate titanate [Pb(Ti,Zr)O_3(PZT)] [25]. A similar result was obtained by Kalyani *et al.* by an *ex situ* technique [26]. More recently, Hinterstein *et al.* have suggested that field-induced phase transformation is the dominant factor in determining the overall piezoelectric strain of a soft PZT [27]. Field-induced phase transformations have also been reported in other ferroelectric systems exhibiting a high piezoelectric response, such as $BiScO_3$-$PbTiO_3$ [28], $BaTiO_3$-based systems [29–31], $Na_{1/2}Bi_{1/2}TiO_3$-based systems [32–34], and (K,Na)NbO_3-based systems [35]. Because of the complications associated with overlapping of Bragg profiles, domain switching studies have mostly been reported for compositions away from the critical MPB, i.e., exhibiting single phase. So far it has not been established how the two phenomena (domain switching and phase transformation) influence each other in the core MPB compositions of piezoelectric alloys. The understanding of this issue is of great fundamental significance since it has direct bearing on our current understanding of the fundamental mechanisms at work in MPB compositions exhibiting a very high piezoelectric response. In the present paper, we have addressed this issue in detail by studying important compositions spanning the $BiScO_3$-$PbTiO_3$ morphotropic phase boundary. Similar to PZT, this alloy system is known for its high piezoelectric performance at the MPB [36]. Our results show that the propensity of domain switching is significantly reduced in the MPB composition as compared to the neighboring non-MPB composition.

II. EXPERIMENT

The details related to the specimen synthesis can be found in Ref. [28]. An *in situ* electric-field high-energy x-ray diffraction (XRD) experiment was carried out at the Advanced Photon Source at Argonne National Laboratory in transmission geometry (beamline 11-ID-C), which ensured

*rajeev@materials.iisc.ernet.in

that the measured diffraction data probe the bulk response of the specimen. A monochromatic beam of a wavelength of 0.111 65 Å and a size of $500 \times 500\,\mu m^2$ was used for the diffraction experiments. The disk-shaped ceramic samples were cut to $10 \times 1 \times 1\,mm^3$ ($l \times b \times t$) dimensions, and an electric field was applied across $10 \times 1\,mm^2$ faces of the sample. Electroding was performed using a silver paste across the surface to which an electric field was applied. The data were collected as a two-dimensional image, wherein, the circular Debye rings correspond to different *hkl* diffracted beams. The schematic details of the *in situ* diffraction geometry is shown in the Supplemental Material Fig. S1 [37]. Ceria (CeO_2) was used as the standard to calibrate the sample to detector distance. The diffraction images were divided into 24 azimuthal sectors of 15° widths with the azimuthal sector most closely oriented to the direction of the applied electric field defined as $\psi = 0°$. The *in situ* electric-field-dependent study is generally carried out by applying a triangular bipolar wave form. The field was varied in incremental steps of 0.16 kV/mm, and the diffraction pattern recorded. The amplitude of the field was 2.5 kV/mm. The piezoelectric strains of the ceramic specimens were measured using a Radiant Premier Precision II setup with an MTI photonic sensor. The direct piezoelectric coefficient was measured with a Berlincourt piezometer (Piezotest PM 300). Le Bail and structural analyses of the diffraction data were carried out using the software package FULLPROF [38].

III. RESULTS

A. Piezoelectric properties of the MPB and the non-MPB compositions

For the field-induced domain switching study two compositions of $(1-x)PbTiO_3$-$(x)BiScO_3$(PT-BS) were investigated: a non-MPB of $x = 0.40$ (BS40) with d_{33} of 260 pC/N and an MPB of $x = 0.3725$ (BS3725) with $d_{33} = 425\,pC/N$. Figure 1 compares the electric-field-dependent longitudinal strain on pellets of the non-MPB and the MPB compositions. As anticipated, at any given field the magnitude of strain of the non-MPB composition is less than that of the MPB composition. For example, at $E = 2.5$ kV/mm, the positive strains are 0.11% and 0.21% for the non-MPB and the MPB compositions, respectively. This is also consistent with the considerably larger d_{33} (as measured by Berlincourt-based piezometer) of the MPB composition as compared to the non-MPB composition, mentioned above.

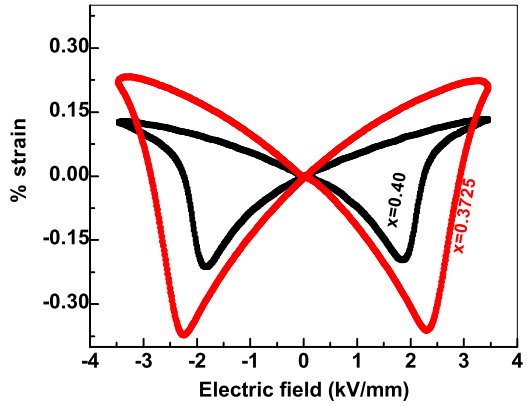

FIG. 1. Strain-field response of (x)BS-$(1-x)$PT for $x = 0.40$ (non-MPB, BS40) and $x = 0.3725$ (MPB, BS3725) measured at 1 Hz.

B. Field-induced domain switching—analysis strategy

The diffraction pattern of the non-MPB composition ($x = 0.40$) shows the pseudocubic $\{111\}_{pc}$ profile to be a doublet and the $\{200\}_{pc}$ pseudocubic profile to be a singlet. These features are consistent with a rhombohedral distortion of the perovskite structure. The XRD pattern of the MPB composition ($x = 0.3725$), on the other hand, suggests a mixture of rhombohedral and tetragonal phases as was originally suggested by Eitel *et al.* [36]. Subsequent studies, using the Ritveld fitting of the full powder-diffraction pattern, reported that a lower-symmetry monoclinic (Cm) structural model, instead of the rhombohedral ($R3m$), fits the diffraction pattern of the MPB and the non-MPB compositions better [28,39–41]. It may however be pointed out that even a close visual inspection of the $\{200\}_{pc}$ profiles of $x = 0.40$ did not reveal any asymmetry in the peak shape as would be anticipated for a monoclinic distortion. A similar scenario occurs in PZT close to the MPB where in the rhombohedral-like diffraction patterns, fit relatively better by considering a monoclinic (Cm) structural model [42]. Since in most of the Rietveld analyses reported before, the microstructural parameters have played an important role in the betterment of the overall fit, we feel that the relatively better fitting of the overall diffraction patterns by invoking a monoclinic structure is because of the availability of the relatively large number of refinable structural (including the thermal/displacement parameters) and microstructural parameters with the monoclinic structural model. For the sake of argument, even if we consider the monoclinic distortion to exist, but too small to show a splitting/asymmetry in the $\{h00\}_{pc}$ profile of $x = 0.40$, one can expect the magnitude of the monoclinic distortion to grow at high fields. This should lead to the development of asymmetry/splitting in the otherwise singlet and symmetric $\{200\}_{pc}$ reflection. Contrary to this, even at a high field of 2.5 kV/mm, the $\{200\}_{pc}$ reflection of the non-MPB composition ($x = 0.40$) exhibits a symmetric singlet profile. We also found the entire diffraction pattern of $x = 0.40$ at a field of 2.5 kV/mm could be perfectly indexed with rhombohedral unit cell (Fig. S2 of the Supplemental Material [37]). These observations suggest that the average structure of the non-MPB composition ($x = 0.40$) remains rhombohedral at all fields. This was also the case for the MPB composition. In view of the above, it is not surprising that domain switching studies on PZT via a diffraction method have been reported by considering the rhombohedral structure [19,20,27], although these very patterns would fit relatively better with the monoclinic structure by Rietveld technique [42]. Furthermore, with regard to a comparative study of the field induced domain switching in the non-MPB and MPB compositions, the subtle structural issues (monoclinic or rhombohedral) are not very relevant since the same analysis approach has been adopted for both the compositions. In view of the above, and for the sake of simplicity, we have limited ourselves by considering rhombohedral ($R3m$) structure for

the non-MPB composition ($x = 0.40$) and the rhombohedral ($R3m$)+ tetragonal ($P4mm$) phase coexistence for the MPB composition ($x = 0.3725$).

On application of the electric field, the domains tend to reorient with spontaneous polarization more closely aligned with the field direction. This phenomenon manifests as a relative change in the intensity of the symmetry-related Bragg peaks. For a rhombohedral phase with polarization along the [111] direction, the electric field would increase the intensity of the $(111)_R$ rhombohedral peak at the expense of the intensity of the $(11\bar{1})_R$ rhombohedral peak. Similarly, for the tetragonal phase whose spontaneous polarization is along $[001]_T$, the intensity of the $(00l)_T$ tetragonal peak would increase at the expense of the intensity of the $(h00)_T$ peak. Here, we assume that the indices of the direction are normal to the plane with the same indices. This assumption is valid for a small rhombohedral/tetragonal distortion from the cubic structure [18,19]. For example, in our case, the rhombohedral angles of the rhombohedral phase in the non-MPB and the MPB compositions are 89.75° and 89.70°, respectively, which is very close to 90°.

In ferroelectric rhombohedral perovskites, the volume fraction of the [111] domains which have been reoriented through the application of the electric field is given by [18,19]

$$\eta_{111} = \frac{\frac{I_{111}}{I'_{111}}}{\frac{I_{111}}{I'_{111}} + 3\frac{I_{11\bar{1}}}{I'_{11\bar{1}}}} - \frac{1}{4},$$

where I_{111} and $I_{11\bar{1}}$ are the integrated intensities of the (111) and $(11\bar{1})$ reflections, respectively, on application of field and I'_{111} and $I'_{11\bar{1}}$ are the integrated intensities of the (111) and $(11\bar{1})$ reflections, respectively, before application of the field. Similarly, for the tetragonal ferroelectric perovskite, the volume fraction of the field-induced domain reorientation is given by

$$\eta_{002} = \frac{\frac{I_{002}}{I'_{002}}}{\frac{I_{002}}{I'_{002}} + 2\frac{I_{200}}{I'_{200}}} - \frac{1}{3},$$

where I_{002} and I_{200} are the integrated intensities of the $(002)_T$ and $\{200\}_T$ reflections, respectively, in the presence of the field. I'_{002} and I'_{200} are the integrated intensities of the $(002)_T$ and $\{200\}_T$ reflections, respectively, before application of the field. Apart from the estimation of the domain reorientation, the shift in the peak positions with the electric field can be used to measure lattice strain [18,19],

$$\varepsilon_{hkl} = \frac{d_{hkl}(E) - d_{hkl}(0)}{d_{hkl}(0)}.$$

C. Domain switching and lattice strains in the MPB and the non-MPB compositions

Figure 2 shows the $\{111\}_{pc}$ and $\{200\}_{pc}$ pseudocubic Bragg profiles at $E = 0$ and $E = 2.5\,\mathrm{kV/mm}$ of the MPB and the non-MPB compositions. The gradual evolution of the Bragg profiles with field and orientation (ψ) with respect to the electric-field direction is given in the Supplemental Material Fig. S3 [37] for the non-MPB composition. As anticipated, for the rhombohedral non-MPB composition, $\{111\}_{pc}$ is a doublet comprising $(111)_R$ and $(11\bar{1})_R$ reflections, and $\{200\}_{pc}$

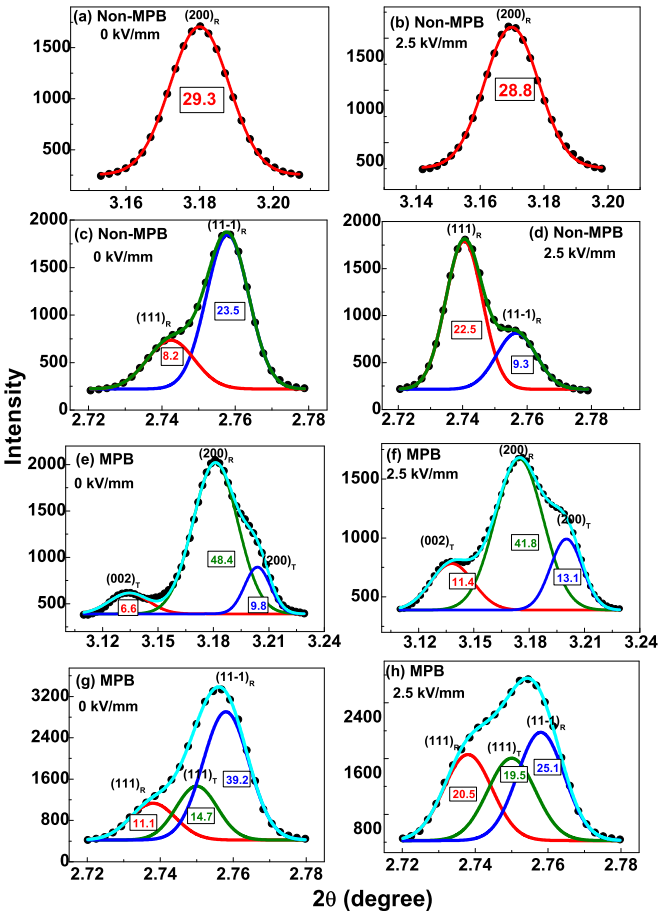

FIG. 2. Fitted Bragg profiles of the pseudocubic $\{111\}_{pc}$ and $\{200\}_{pc}$ of the non-MPB (a)–(d) and the MPB composition (e)–(h) at 0 kV/mm (unpoled sample) and 2.5 kV/mm. The raw data are represented by dots. The peak positions were verified independently by Rietveld analysis. The area (integrated intensity) of the individual profiles, used for fitting the total profile, is given beneath the peak of the corresponding profile. The subscripts R and T refer to rhombohedral and tetragonal indices, respectively.

is a singlet [rhombohedral index $(200)_R$]. For the MPB composition, $\{200\}_{pc}$ is a triplet. The peaks on the extreme left and the extreme right correspond to $(002)_T$ and $(200)_T$ of the tetragonal phase, and the one in the middle corresponds to the $(200)_R$ of the rhombohedral phase. Although, in principle, the $\{111\}_{pc}$ of the MPB is a triplet, comprising $(111)_R$, $(11\bar{1})_R$, and $(111)_T$, the observed $\{111\}_{pc}$ profile appears as a doublet. A full profile analysis undertaken on the MPB composition using Rietveld refinement revealed that the $(111)_T$ profile of the tetragonal phase overlaps severely with the $(11\bar{1})_R$ profile of the rhombohedral phase. For details, please refer to Fig. S4 of the Supplemental Material [37]. For calculation of the domain switching fractions, the integrated intensities of the $(111)_T$, $(002)_T$, and $(200)_T$ profiles of the tetragonal phase and the $(111)_R$, $(11\bar{1})_R$, and $(200)_R$ profiles of the rhombohedral phase were obtained by keeping the peak positions close to that as obtained from the Rietveld fit and by keeping the full width at half maximum values nearly the same. This strategy led to a systematic field dependence of the domain switching fraction and lattice strains of the coexisting phases. On application

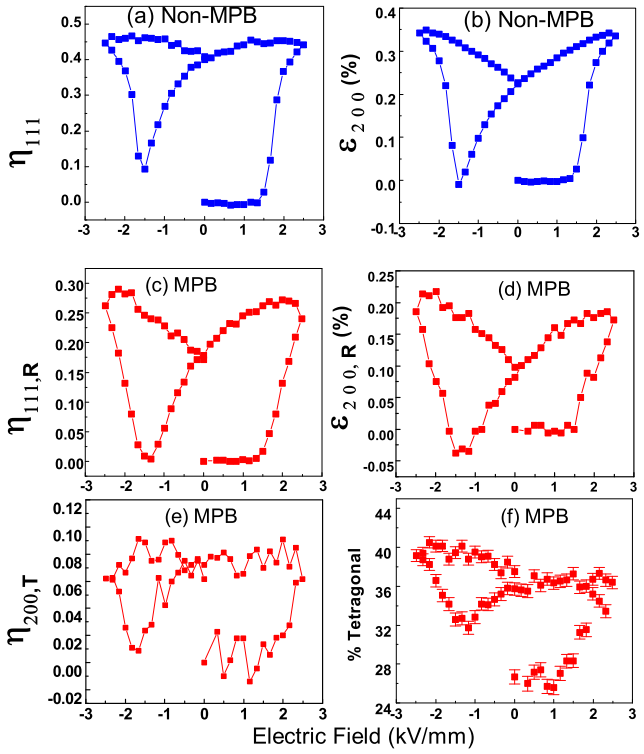

FIG. 3. Electric-field dependence of (a) the rhombohedral 111 domain switching fraction of BS40, (b) the rhombohedral 200 lattice strain of BS40, (c) the rhombohedral 111 domain switching fraction of BS3725, (d) rhombohedral 200 lattice strain of BS3725, (e) the tetragonal 002 domain switching fraction of BS3725, and (f) the tetragonal phase fraction of BS3725.

of a high field, the two visibly perceptible changes in the profiles of the non-MPB composition are: (i) a reversal in the intensity ratio of the $(111)_R$ and $(11\bar{1})_R$ reflections, and (ii) a shift in the Bragg peak position of the $(200)_R$ peak. In fact, both these quantities depend on the orientation (ψ) of the plane normal with respect to the electric field (for details refer to Fig. S5 in the Supplemental Material [37]) with their maximum values along the longitudinal direction, i.e., $\psi = 0^\circ$. In this paper, we will therefore concern ourselves with values of η and ε corresponding to $\psi = 0^\circ$. Figures 3(a) and 3(b) show the field dependence of $\eta_{111,R}$ and $\varepsilon_{200,R}$ of the non-MPB composition. Both quantities show hysteresis with field cycling. At 2.5 kV/mm, $\varepsilon_{200,R}$(=0.32%) is nearly five times larger than $\varepsilon_{111,R}$(=0.07%). A similar result by Guo *et al.* on a rhombohedral PZT close to the MPB was interpreted as a structural proof of the mechanism associated with large piezostrain parallel to nonpolar directions of the crystal [8]. However, stresses associated with non-180° domain walls as well as intergranular strains in ferroelectric ceramics can also lead to such asymmetric distortions of specific (*hkl*) peaks [18,19,43].

For the MPB composition, which comprises tetragonal and rhombohedral phases, at $E = 2.5$ kV/mm, the largest lattice strain was still found for the $(200)_R$ of the rhombohedral phase (i.e., $\varepsilon_{200,R} \sim 0.20\%$). The second largest lattice strain is for the $(111)_T$ of the tetragonal phase ($\varepsilon_{111,T} = 0.10\%$). Lattice strains for $(200)_T$, $(002)_T$, $(111)_R$, and $(11\bar{1})_R$ are less than 0.05%. The field dependence of the switching fraction of the tetragonal domains (η_{002}), rhombohedral domains (η_{111}), and $\varepsilon_{200,R}$ lattice strain of the coexisting *R* phase of the MPB composition is shown in Figs. 3(c)–3(e). We note that maximum $\varepsilon_{200,R}$(0.20%) for the MPB composition [Fig. 3(d)] is nearly half the value of the non-MPB composition (0.35%) [Fig. 3(b)]. Similarly, the rhombohedral domain switching fraction in the MPB composition [η_{111}(MPB) = 0.28%] is also significantly smaller as compared to that in the non-MPB composition [η_{111}(non-MPB) = 0.45]. The fact that the $\varepsilon_{200,R}$ lattice strain is reduced along with the reduction in the domain switching propensity in the MPB composition reinforces the fact that the two phenomena are interrelated [43].

D. Field-induced phase transformation

Lalitha *et al.* have earlier shown evidence of field-induced phase transformation in the MPB composition of this system [28]. We estimated the phase fractions as a function of the field using two different approaches. It was found that for the non-MPB rhombohedral composition ($x = 0.40$), the integrated intensity of the $(200)_R$ profile remains almost unchanged even while the relative intensities of the $(111)_R$ and $(11\bar{1})_R$ profiles changed dramatically due to field-induced preferred orientation. In view of this, the change in the integrated intensity of the rhombohedral $(200)_R$ profile of the MPB composition can be related to the change in the relative volume fraction of the rhombohedral phase by the electric field. Since the intensity (integrated area) of a Bragg peak is directly proportional to the volume fraction of the phase, it is possible to create a calibration relating the integrated intensity of the rhombohedral $(200)_R$ peak and volume fraction of the rhombohedral phase. The intensity of $(200)_R$ would be zero if the rhombohedral phase is absent. The other point of the linear calibration was determined by correlating the area of the rhombohedral $(200)_R$ of the MPB composition with the volume fraction determined by Rietveld analysis of the unpoled specimen which is free from preferred orientation (please refer to Fig. S4 of the Supplemental Material [37]). The resulting calibration graph is shown in the Supplemental Material Fig. S6 [37]. Figure 3(f) shows the volume fraction of the coexisting tetragonal phase as a function of the cyclic electric field. We may note that the value of the tetragonal fraction was found to be consistent with the tetragonal phase fraction determined independently using the area of the tetragonal $(111)_T$ profile [assuming the intensity of $(111)_T$ does not change noticeably with the preferred orientation in the tetragonal phase]. The tetragonal fraction varied from ~25% (before application of the field) to ~40% (at 2.5 kV/mm). We also determined the phase fractions using the conventional Rietveld analysis (by invoking the preferred orientation parameters) and found similar values of phase fractions (Figs. S7 and S8 of the Supplemental Material [37]). Except for the fact that the tetragonal volume fraction increases with the field in PT-BS [28], whereas it decreases in PZT [25,26], the hysteresis in the volume fraction obtained by us is similar to what was reported earlier by Hinterstein *et al.* for PZT using a special orientation of the specimen with respect to the electric field and the beam direction to avoid the preferred orientation effect [25].

IV. DISCUSSION

In general, due to the ferroelectric-ferroelectric instability at the MPB, it is anticipated that the crystallographic anisotropy of the polarization direction would vanish, or significantly reduced, as the critical MPB composition is approached. Concomitantly, the domain wall energy of the MPB composition is also expected to be considerably reduced, leading to its enhanced motion/displacement as compared to that in the compositions away from the critical MPB [11]. Although it is well known that the piezoelectric properties are maximum for critical MPB compositions in different ferroelectric alloy systems, at present there is a lack of a systematic study of the domain switching fraction across the MPB. Ghosh *et al.* have shown a one-to-one correspondence between the propensity of domain switching and the dielectric and piezoelectric responses in a $BaTiO_3$ ceramic of varying grain sizes. In this study, the authors attributed the enhanced propensity of domain switching to enhanced domain wall displacement. In view of this, the significantly reduced domain switching fraction ($\eta = 0.28$) in the MPB composition, as compared to the non-MPB composition ($\eta = 0.45$) of our system, would imply that the domain wall motion is considerably impeded at the MPB. This result contradicts the domain wall displacement-based arguments, according to which the enhanced piezoelectric response of critical MPB compositions is associated with higher domain wall displacements. We argue that the phenomenon in MPB systems is much more complex. In a polycrystalline ferroelectric ceramic of MPB composition, each grain has regions of two or more ferroelectric phases, separated by interphase boundaries. And within a given ferroelectric region, ferroelectric domains, separated by domain walls, are expected to be present. On application of an electric field two phenomena are expected to happen together: (i) one ferroelectric phase grows at the cost of the other, and (ii) the domains within a given phase would tend to align, leading to domain wall motion. Both phenomena cannot be expected to be independent of each other. Our observation of the volume fraction of the tetragonal phase growing at the cost of the rhombohedral phase on application of an external field can be imagined to occur in two different ways: (i) the additional tetragonal phase nucleates and grows within the rhombohedral phase region, and (ii) the already existing tetragonal-rhombohedral phase boundary advances into the rhombohedral phase region. With regard to the first mechanism, i.e., the additional tetragonal phase nucleating and growing inside the rhombohedral phase region, the preferred site for nucleation of the tetragonal phase within the rhombohedral region is most likely to be the domain walls. This argument is based on the phase field simulation study by Rao and Wang in which the authors demonstrate that nuclei of a new ferroelectric phase can grow in the domain wall regions on application of an electric field [15]. In this scenario, only those regions of the domain walls where nucleation of the tetragonal phase has not happened, will respond to the electric field by displacing themselves so as to effect domain switching. In contrast, when field-induced structural transformation does not take place in a given ferroelectric system, the role of the applied electric field is primarily to effect domain switching. Although crude, this model can explain why the non-MPB composition, in which the electric field does not induce structural transformation, can exhibit a higher domain switching fraction as compared to the MPB composition. The next question that naturally arises is—what makes for the enhanced piezoelectric response of the MPB composition despite the reduced domain wall displacement? Hinterstein *et al.* have analyzed the strain contributions due to domain switching, lattice strain, and phase transformation for a MPB composition of PZT [27]. The authors concluded that the nearly 80% of piezoelectric strain is contributed by field-induced structural transformation. Since field-induced rhombohedral to tetragonal transformation is evident in our MPB composition as well, we can argue that, despite the reduced domain wall motion in the critical MPB composition, the large piezoelectric response arises primarily due to the field-induced transformation. Very recently, Fan *et al.* have used the same experimental technique as ours to investigate domain switching behavior in $Pb(Zr_{0.535}Ti_{0.465})O_3$ [44]. The authors reported that after the first poling, the structure transformed from tetragonal to monoclinic and that this transformed phase was stable even after removal of the field. In the absence of the bipolar diffraction data it is not possible to ascertain if this stability is sustained or not when the field direction is reversed. However, similar to our case, the authors determined the domain switching fraction as a function of the field and reported that the monoclinic phase shows reduced domain switching as compared to the other phases. It is however not clear if the composition $Pb(Zr_{0.535}Ti_{0.465})O_3$ chosen by the authors corresponds to the most critical composition, exhibiting the maximum piezoelectric response, or not. If not, we feel that one should be cautious to extrapolate the results of the noncritical composition to understand the mechanism associated with the most critical MPB composition, exhibiting a very large piezoelectric response, as the phenomenon may be qualitatively different in both cases. In our case, we have directly investigated the mechanism associated with the most critical MPB composition of $PbTiO_3$-$BiScO_3$ to suggest that field-induced transformation is the primary factor for the large piezoelectric response.

V. CONCLUSIONS

In conclusion, a comparative *in situ* electric-field-dependent high-energy synchrotron x-ray diffraction study on a critical MPB and a close by non-MPB composition of the high-performance piezoelectric alloy $BiScO_3$-$PbTiO_3$ revealed that the rhombohedral ferroelectric-ferroelastic domain switching fraction is considerably reduced in the MPB composition as compared to the non-MPB composition. The reduced domain switching is also accompanied by a corresponding reduction in the field-induced lattice strain along the nonpolar direction suggesting a strong connection between the two phenomena. The MPB composition exhibits electric-field-induced phase transformation, whereas the non-MPB composition does not, thereby suggesting that the hindrance to the domain wall motion in the MPB is likely to be related to the field-induced phase transformation. Our results also favor the idea that field-induced transformation is most likely to be the dominant mechanism responsible for the large piezoelectric response in the critical MPB compositions of ferroelectric ceramics.

ACKNOWLEDGMENTS

R.R. acknowledges the Science and Engineering Research Board of the Department of Science and Technology, Government of India, for providing financial assistance (Grant No. SERB/F/5046/2013-14). R.R. also acknowledges fruitful discussion with Dragan Damjanovic.

[1] V. A. Isupov, Sov. Phys.-Solid State **10**, 989 (1968).
[2] J. Y. Li, R. C. Rogan, E. Üstündag, and K. Bhattacharya, Nature Mater. **4**, 776 (2005).
[3] H. Fu and R. E. Cohen, Nature (London) **403**, 281 (2000).
[4] L. Bellaiche, A. García, and D. Vanderbilt, Phys. Rev B **64**, 060103(R) (2001).
[5] D. Vanderbilt and M. H. Cohen, Phys. Rev. B **63**, 094108 (2001).
[6] A. J. Bell, J. Appl. Phys. **89**, 3907 (2001).
[7] D. Damjanovic, J. Am. Ceram. Soc. **88**, 2663 (2005).
[8] R. Guo, L. E.Cross, S.-E. Park, B. Noheda, D. E. Cox, and G. Shirane, Phys. Rev. Lett. **84**, 5423 (2000).
[9] B. Noheda, D. E. Cox, G. Shirane, S.-E. Park, L. E. Cross, and Z. Zhong, Phys. Rev. Lett. **86**, 3891 (2001).
[10] M. Budimir, D. Damjanovic, and N. Setter, Phys. Rev. B **73**, 174106 (2006).
[11] Y. M. Jin, Y. U. Wang, A. G. Khachaturyan, J. F. Li, and D. Viehland, Phys. Rev. Lett. **91**, 197601 (2003).
[12] Y. M. Jin, Y. U. Wang, A. G. Khachaturyan, J. F. Li, and D. Viehland, J. Appl. Phys. **94**, 3629 (2003).
[13] Y. U. Wang, Phys. Rev. B **76**, 024108 (2007).
[14] Y. U. Wang, Phys. Rev. B **73**, 014113 (2006).
[15] W.-F. Rao and Y. U. Wang, Appl. Phys. Lett. **90**, 041915 (2007).
[16] K. A. Schönau, M. Knapp, H. Kungl, M. J. Hoffmann, and H. Fuess, Phys. Rev. B **76**, 144112 (2007).
[17] G. Tutuncu, D. Damjanovic, J. Chen, and J. L. Jones, Phys. Rev. Lett. **108**, 177601 (2012).
[18] J. L. Jones, M. Hoffman, J. E. Daniels, and A. J. Studer, Appl. Phys. Lett. **89**, 092901 (2006).
[19] A. Pramanick, D. Damjanovic, J. E. Daniels, J. C. Nino, and J. L. Jones, J. Am. Ceram. Soc. **94**, 293 (2011).
[20] D. A. Hall, A. Steuwer, B. Cherdhirunkorn, T. Mori, and P. J. Withers, Acta Mater. **54**, 3075 (2006).
[21] M. J. Hoffmann, M. Hammer, A. Endriss, and D. C. Lupascu, Acta Mater. **49**, 1301 (2001).
[22] L. Daniel, D. A. Hall, K. G. Webber, A. King, and P. J. Withers, J. Appl. Phys. **115**, 174102 (2014).
[23] J. L. Jones, E. Aksel, G. Tutuncu, T.-M. Usher, J. Chen, X. Xing, and A. J. Studer, Phys. Rev. B **86**, 024104 (2012).
[24] D. Ghosh, A. Sakata, J. Carter, P. A. Thomas, H. Han, J. C. Nino and J. L. Jones, Adv. Funct. Mater. **24**, 885 (2014).
[25] M. Hinterstein, J. Rouquette, J. Haines, P. Papet, M. Knapp, J. Glaum, and H. Fuess, Phys. Rev. Lett. **107**, 077602 (2011).
[26] A. K. Kalyani, Lalitha K. V., A. R. James, A. N. Fitch, and R. Ranjan, J. Phys.:Condens. Matter **27**, 072201 (2015).
[27] M. Hinterstein, M. Hoelzel, J. Rouquette, J. Haines, J. Glaum, H. Kungl, and M. Hoffman, Acta Mater. **94**, 319 (2015).
[28] Lalitha K. V., A. N. Fitch, and R. Ranjan, Phys. Rev. B **87**, 064106 (2013).
[29] A. K. Kalyani, H. Krishnan, A. Sen, A. Senyshyn, and R. Ranjan, Phys. Rev. B **91**, 024101 (2015).
[30] A. K. Kalyani, D. K. Khatua, B. Loukya, R. Datta, A. N. Fitch, A. Senyshyn, and R. Ranjan, Phys. Rev. B **91**, 104104 (2015).
[31] K. Brajesh, K. Tanwar, M. Abebe, and R. Ranjan, Phys. Rev. B **92**, 224112 (2015).
[32] B. N. Rao, R. Datta, S. S. Chandrashekaran, D. K. Mishra, V. Sathe, A. Senyshyn, and R. Ranjan, Phys. Rev. B **88**, 224103 (2013).
[33] R. Garg, B. N. Rao, A. Senyshyn, P. S. R. Krishna, and R. Ranjan, Phys. Rev. B **88**, 014103 (2013).
[34] R. Garg, A. Senyshyn, and R. Ranjan, J. Appl. Phys. **114**, 234102 (2013).
[35] T. Iamsasri, G. Tutuncu, C. Uthaisar, S. Wongsaenmai, S. Pojprapai, and J. L. Jones, J. Appl. Phys. **117**, 024101 (2015).
[36] R. E. Eitel, T. R. Shrout, and C. A. Randall, J. Appl. Phys. **99**, 124110 (2006).
[37] See Supplemental Material at http://link.aps.org/supplemental/10.1103/PhysRevB.93.104103 for the schematic details of the *in situ* diffraction geometry.
[38] R.-J. Carvajal, *FULLPROF. A Rietveld Refinement and Pattern Matching Analysis Program* (Laboratories Leon Brillouin (CEA-CNRS), France, 2000).
[39] B. Kim, P. Tong, D. Kwon, J. M. S. Park, and B. G. Kim, J. Appl. Phys. **105**, 114101 (2009).
[40] K. Datta, D. Walker, and P. A. Thomas, Phys. Rev. B **82**, 144108 (2010).
[41] T. Hungria, F. Houdellier, M. Alguero, and A. Castro, Phys. Rev. B **81**, 100102 (2010).
[42] Ragini, R. Ranjan, S. K. Mishra, and D. Pandey, J. Appl. Phys. **92**, 3266 (2002).
[43] Lalitha K. V., C. M. Fancher, J. L. Jones, and R. Ranjan, Appl. Phys. Lett. **107**, 052901 (2015).
[44] L. Fan, J. Chen, Y. Ren, Z. Pan, L. Zhang, and X. Xing, Phys. Rev. Lett. **116**, 027601 (2016).